Engineering Chemistry
ISSN: 2813-6535, Vol. 7, pp 89-98
doi:10.4028/p-GI7wfs

Submitted: 2023-12-02
Revised: 2023-12-25
Accepted: 2023-12-29
Online: 2024-06-26

Highly Porous Ni Electrode Decorated with Fe_3O_4 for Oxygen Evolution Reaction (OER)

Bayu Satriya Wardhana[1,2,a*], Sheng-Wei Lee[2,3,b], Shian-Ching Jang[2,4,c]

[1]Department of Mechanical Engineering, Brawijaya University, Malang City, 65145, Indonesia

[2]Institute of Material Science and Engineering, National Central University, Taoyuan City, 32001 Taiwan, ROC

[3]Department of Chemical and Material Engineering, National Central University, Taoyuan City, 32001, Taiwan, ROC

[4]Department of Mechanical Engineering, National Central University, Taoyuan City, 32001 Taiwan, ROC

[a]wardhanabayu@ub.ac.id, [b]swlee@g.ncu.edu.tw, [c]jscjang@ncu.edu.tw

Keywords: nickel porous structure, oxygen evolution reaction, laser calcination, Fe_3O_4 catalyst

Abstract. Hydrogen is an environmentally friendly energy source that can be extracted from water through electrolysis. However, the slow oxygen evolution reaction (OER) at the anode side is the main obstacle to the widespread use of water-splitting devices. This study used self-developed highly porous nickel structures(SMNF) and commercial nickel foam(CNF) as working electrodes in the electrolysis process. Iron(II, III) Oxide (Fe_3O_4) as a catalyst is coated with a dip coating technique on the Ni porous structure and then calcined using a laser process to produce a Ni-Fe_3O_4-based electrode. Electrochemical test results show that the presence of Fe_3O_4 significantly impacts high reaction kinetics. The SMNF-Fe_3O_4 demonstrated an overpotential of 217.3 mV at 1 M KOH electrolyte, at a current density of 10 mA, lower to SMNF electrode without Fe_3O_4 with an overpotential of 361.4 mV under the same conditions. In addition, the difference in porosity less significantly affects the electrode's effectiveness due to the slight difference in mass loading, which is only < 5 mg. However, electro-impedance spectroscopy(EIS) testing shows better performance on SMNF-Fe_3O_4 with a smaller electrical series resistance (ESR), around 0.638 Ω, compared to CNF-Fe_3O_4, which is 0.767 Ω. Overall, observations by chronoamperometry test at an overpotential of 155 mV at 5 hrs show stable performance of SMNF-Fe_3O_4 electrodes.

Introduction

Hydrogen is a clean energy source that has become increasingly popular in recent years and is expected to be used as an alternative to fossil fuels [1]. Up to 95% of all hydrogen produced is "grey hydrogen," which is produced by the cracking of non-renewable fossil fuels and high carbon emissions [2], [3]. On the other hand, "green hydrogen," or hydrogen produced with a low residual carbon by electrolysis, accounts for just around 4% [3]. This fact occurs for efficiency reasons [4], [5], so increasing the efficiency of producing hydrogen through electrolysis is essential to raising the percentage of "green hydrogen" [6]. To raise green hydrogen production, electrodes with high electrocatalytic activity and economical price are essential in water-splitting. One of the main problems with water electrolysis is that the anode's oxygen evolution reaction (OER) is sluggish [7]. The OER consists of four steps, with one electron connected every step, whereas the hydrogen evolution reaction (HER) is more simply processed with a two-electron-transfer reaction. Consequently, the OER typically demonstrates slow kinetics and requires a bigger overpotential than the HER [8]. Therefore, one of the main goals in research in developing water-splitting devices is to develop and investigate electrodes with high-performance OER, which can increase efficiency.
According to the findings of several studies [8], the characteristics listed below must be possessed by an effective catalyst for the OER process: 1) low cost and earth abundance; 2) no environmental pollution; 3) excellent performance comparable to noble metal-based materials; 4) superior durability and long-term stability; 5) good conductivity; and 6) ease of shape-controlled synthesis. Nickel-based

electrocatalysts are a cheap and effective option for water electrolysis [9], [10]. They are stable and work well as electrocatalysts for HER and OER. [11]. Nickel exhibits favourable characteristics as an electrocatalyst due to its notable attributes, including elevated conductivity, thermal stability, and commendable electrical qualities [12]. Typically, nickel (Ni) exists as a divalent cation, although it can adopt various valences within the range of -1 to +4 [13]. This characteristic enables it to undergo a range of electronic transitions. In order to enhance the electrocatalytic performance of nickel materials, it is crucial to manipulate their chemical environment, structure, and morphology carefully [14], [15]. Several factors influence an electrocatalyst's effectiveness in water electrolysis, including its chemical composition, surface chemistry, crystalline structure, porosity, size distribution, and electrical conductivity [13]. As a result, a significant amount of research has been conducted on the development of electrocatalysts based on nickel for water electrolysis. Porous catalysts can be created using a high porous structure to improve active site exposure to electrolytes.

The presence of iron (II, III) oxide (Fe_3O_4) to form NiFe-based materials is one of the most promising OER catalysts due to their availability and high intrinsic activity [8], [16]. Koper and his colleagues conducted a comprehensive theoretical and experimental investigation to investigate the possible relationship between the activities of nickel-based double hydroxides toward oxygen evolution and the natures of the transition metals that were added to alkaline environments [17]. According to their findings, Mn and Fe have almost ideal binding energies, which lowers the predicted OER overpotential. Furthermore, Ni-Fe-based electrocatalysts have several advantages such as high activity and stability, tuning the electronic structure, cheap, and facilitating gas evolution [10]. Motivated by the previous achievements of Ni−Fe-oxide electrocatalysts, which demonstrate stability and capability for water splitting process in an alkaline environment [18], we developed a high-performance and low-cost Ni porous structure with surface-decorated Fe_3O_4 particle electrodes. Laser calcination with low power is used to deposit Fe_3O_4 particles over the porous structure of Ni. The large porosity of the Ni structure is expected to maximize the loading of Fe_3O_4 so that the area for electrochemical activity increases and improves the OER performance.

Experimental Section

The research began by producing highly porous structures from nickel powder as described in schematic Fig.1. Self-manufactured nickel foam (SMNF) is produced by pressing Ni powder in the hydraulic cylinder with 6-ton force in 3 cm diameter dies. After this process, the green body was sintered in an H_2 environment at 600 ℃ for 2 hrs to avoid oxidation, then cut the specimen into 2 cm x 1 cm large. This research also uses commercial Ni foam with a porosity of > 95% as a comparison to determine the tendency of porosity to electrochemical performance.

Fig. 2 shows the $NiFe_3O_4$ electrocatalyst fabrication process, which is started by immersing a 1cm x 1cm highly porous nickel area in 0.5 M Fe_3O_4 solution for one hour. The Fe_3O_4 solution was created by mixing deionized water with $Fe(NO_3)_3 \cdot 9\ H_2O$, maintained at 45℃ and stirred at constant speed at 400 rpm for 30 minutes. The sample was dried in a vacuum oven at 60℃ and ready for laser calcination. This research uses a low-power laser of 1 watts at an 18.5 cm distance and a 20 times/cycle scanning rate to keep the surface from overheating. The vacuum chamber is kept at 5.7 x 10^{-2} bar to avoid contamination. Weighing is done on the sample before and after dip coating and after the laser calcination to get an overview of the mass loading of the oxide material over a nickel porous structure.

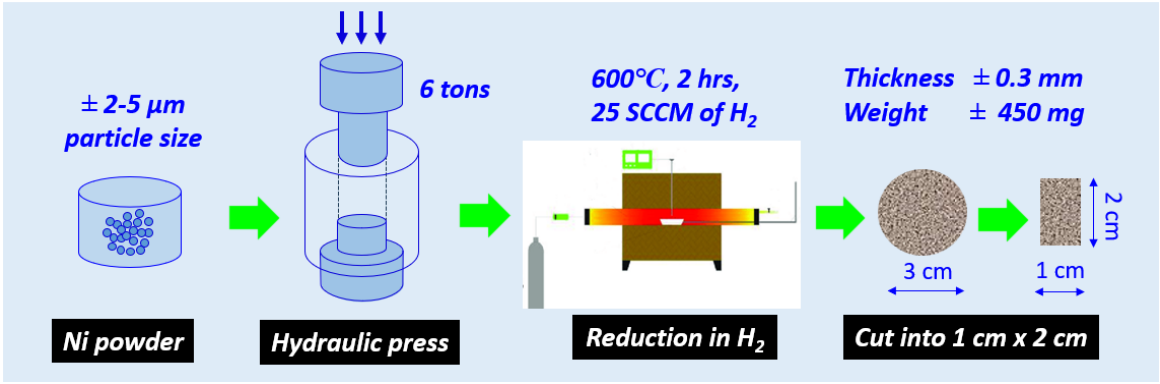

Fig. 1. Schematic picture of SMNF manufacturing

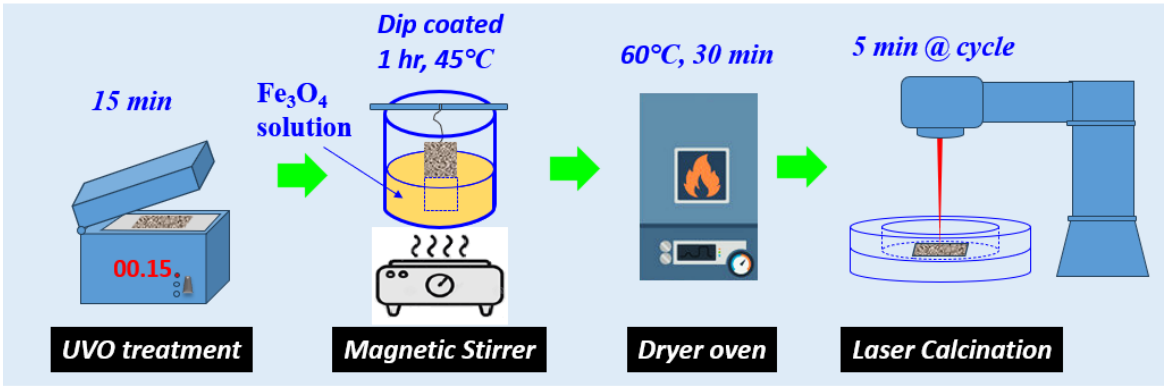

Fig. 2. Schematic picture of SMNF-Fe_3O_4 electrode manufacturing

The phase analysis of NF-Fe_3O_4 electrocatalyst was determined using an X-ray diffractometer (XRD, Bruker, D8A) with monochromatic Cu Kα radiation and a diffraction angle of 20º to 80º. In this research, we optimized the XRD result from our previous study, which uses the same method (laser calcination) to deposit active High Entropy Oxide (HEO) materials on nickel foam for supercapacitor applications[19]. To evaluate the application potential of Ni-Fe_3O_4 electrodes in alkaline electrolyzers, a BioLogic Electrochemical Workstation SP-150 performed electrochemical tests with a 1 cm^2 sample in a high-concentration electrolyte (1 M KOH) at room temperature. The test was carried out with a three-electrode system with Ni-Fe_3O_4 as the working electrode, while Ag/AgCl and Pt were used as reference and counter electrodes, respectively. A constant voltage (CV) test with a scan rate of 100 mV s^{-1} and linear sweep voltammetry (LSV) with scanning rates of 2 mV s^{-1} was employed to measure the complete polarisation curves of the oxygen evolution reaction (OER). The potential window for the CV test was between 0.377 ~ and 0.577 (V vs Ag/AgCl), while for the LSV, it was between -1.00 ~ and 0.800 (V vs Ag/AgCl), as used by several previous studies [8]. Tafel plots are then made based on the LSV test results to determine how sensitive the current response is to overpotential and provide information on the reaction mechanism and rate-limiting steps. The following equation (Eq. 1) calculates the electrochemical surface area (ECSA) based on double layer capacitance methods:

ECSA = Double layer capacitance (CdI) / Specific capacitance (C_s) (1)

The double-layer capacitance (CdI) value is obtained from the anodic slope on the scan rate vs current density plot, while the specific capacitance (C_s) is calculated via the CV curve through the Eq. (2):

$$C_s = \frac{A}{2kmΔV} \quad (2)$$

A is the area under the I-V curve, k is the scan rate (mV s^{-1}), m is an active mass of oxide material (mg), and ΔV is a potential window (mV). In addition, for double-layer capacitance measurements, we set the potential window to a width of 0.1 mV, namely between 0.377 ~ and 0.477, in order to obtain a CV response without a Faradaic reaction at the electrode-electrolyte, so that a more precise

measurement is obtained [12]. However, in actual observations, we had difficulty calculating the specific capacitance value precisely because the response of the measurements was inconsistent. McCrory et al. reported in their benchmarking publications that the C_s values for different metal catalysts varied between 0.022 and 0.130 mF cm^{-2} in alkaline solutions [20]. This report uses most often the value of the C_s about 0.040 mF cm^{-2}, as used by several research studies [20], [21].

Result and Discussion

1. Characterization of Ni-Fe_3O_4 Electrocatalyst

Fig. 3 shows the XRD results of laser calcination of the HEO element over the SMNF structure. We can find a sharp peak (shown with the star symbol) at about 30°, 35°, 43°, and 57° can be indexed as (220), (222), (400), and (551) planes. These diffraction peaks were identified as pure Fe_3O_4 phases (JCPDS card no. 01-071-6336)[22]. The triangle symbol indicates the spinel structure of Mn-Fe_2O_4 according to JCPDS card no. 10-0319. It belongs to a space group of Fd-3m with cell parameter a = 8.499 Å[23]. Other structures indicated by a dot symbol are identified as spinel structures of Mn_3O_4 according to JCPDS card no. 75-0765[24]. The presence of Mn in the XRD results is understandable because, in our previous studies, MnO was one of the dominant elements in HEO. After all, it has good capacitive properties, making it suitable for supercapacitor applications.

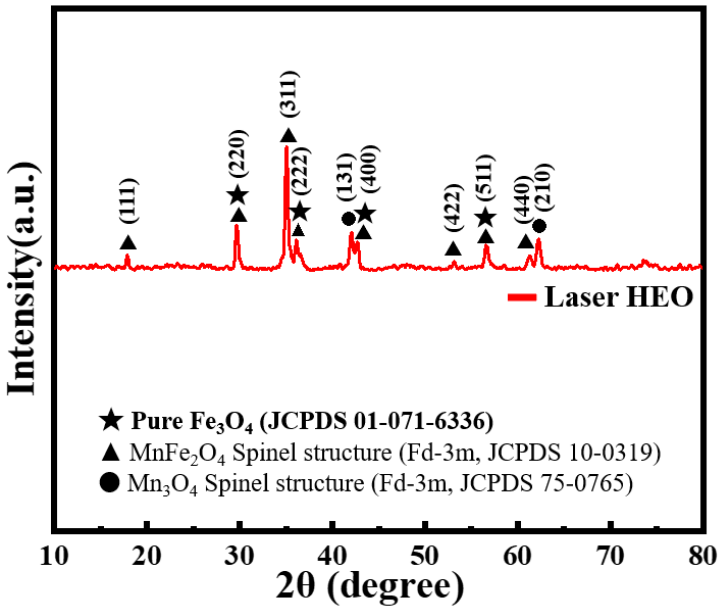

Fig. 3. XRD result of SMNF-Fe_3O_4 electrode

Fig. 4 shows the observations on the porous nickel foam with an optical microscope at low magnifications. Visually, it can be seen that CNF has a rougher surface compared to SMNF, as seen in Fig. 4(a). Observation using optical microscopy shows striking differences in the pore sizes of the electrodes used in this study. The SMNF structure shows uniform porosity with a smaller pore size than the CNF structure. From measurements carried out, CNF has an average porosity of ca. ± 125-150 µm (Fig. 4.b), while SMNF has an average porosity of ca. 10-20 µm (Fig. 4.c). This difference in porosity shows that at the same area (1 cm^2), the SMNF structure has a much larger active surface area, so it has an excellent opportunity to bind the Fe_3O_4 particle as an active material.

Further investigation shows that the SMNF structure has many isolated/closed pores (Fig. 5). These pores allow the Fe_3O_4 solution to have difficulty accessing the structure below the surface and during electrochemical tests, where it will be difficult for the electrolyte to reach parts below the surface. However, in Table 1, we can see that the increase of active material mass due to the differences in porosity is not too significant (less than 5 mg). This fact shows that extensive access to the surface area does not guarantee that the oxide solution can stick optimally to the electrode surface. This incident was possible due to several factors apart from the porosity factor, including (1) the binder

not being used in the coated oxide solution, (2) an inappropriate molar solution, and (3) the electrode surface being hydrophobic. Overall, there is still an opportunity to prove the effect of porosity on performance by improving the pores' structure and manufacturing parameters.

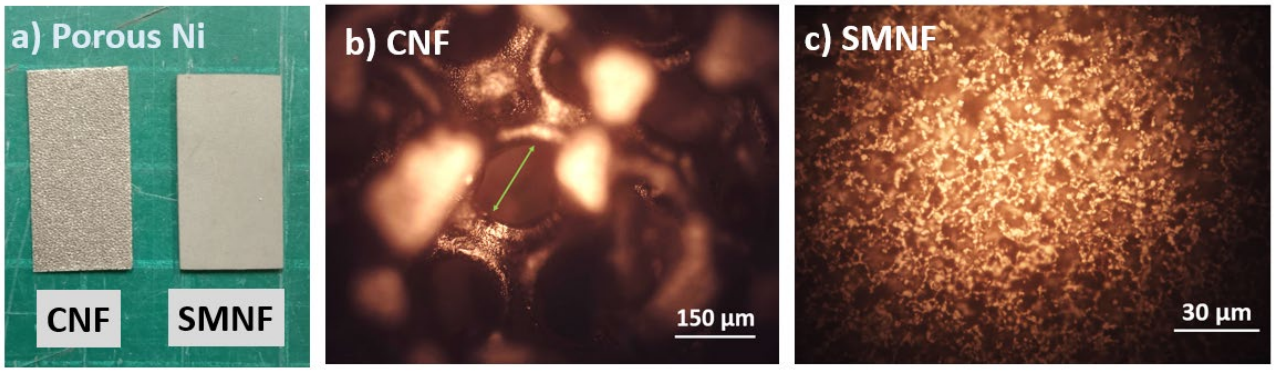

Fig. 4. Optical Microscope of Ni porous structure

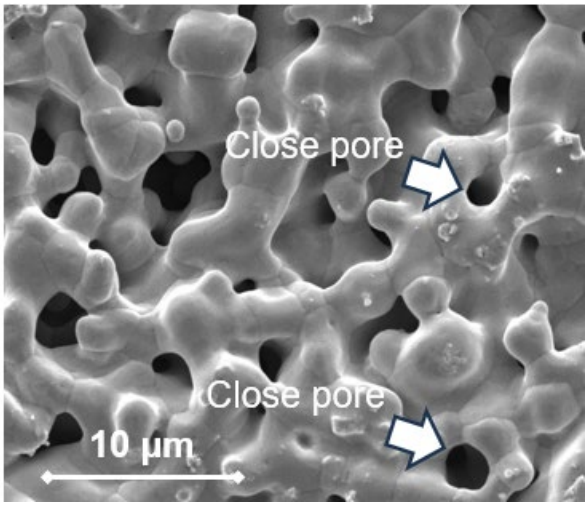

Fig. 5. SEM image of SMNF structure

Table 1. Sample weight during manufacturing

Sample name	Before Dip Coate (mg)	After Laser Calcination (mg)	Mass Loading (mg)
CNF-Fe_3O_4	232.3	236.0	3.7
SMNF-Fe_3O_4	445.8	451.8	6.0

2. Electrochemical performance for OER

Fig. 6(a) shows the CV curve of the SMNF and CNF electrodes, with and without Fe_3O_4. All CV curves have a quasi-rectangular shape, with very sharp edges, without redox peaks, and a shape that tends to be symmetrical and exhibits good electrochemical reversibility. The presence of the Fe_3O_4 element makes the peak current density higher than electrodes without additional active material, as seen from the response curve, which shifts upwards at the tip. The curves on electrodes with additional active material are similar, meaning the electrodes have similar electrocatalytic properties. In addition, the interaction between Ni and Fe is essential to increase OER activity. According to Chai et al.[25], Fe doping encourages the chemisorption of oxygen-containing intermediates, which raises OER activity. While according to Boettcher et al.[26], Fe activates Ni centres by inducing a partial charge-transfer process.

Fig. 6(b) demonstrates the linear sweep voltammetry (LSV) test at the scan rate value of 10 mV s^{-1}. From this figure, we can see that LSV curves show that the SMNF-Fe_3O_4 electrodes in the 1 M KOH electrolyte solution achieve an overpotential of about 271 mV at a current density of 10 mA cm^{-2},

lower than the SMNF electrode without Fe_3O_4 catalyst overpotential with 361.4 mV, and become superior to the other electrode used in this research. However, the results are comparable to similar research that utilized Ni-Fe alloy as an electrode in the water separation process [11], [18]. In addition, the influence of the material's porosity, which is expected to provide the maximum effect due to an enormous surface area, is less pronounced because the difference in mass loading is too small (less than 5 mg). The low absorption of the SMNF structure towards metal oxide is possible because some of its structures tend to be closed pores/dead pores, as can be seen in the SEM test results in Fig. 5, which means that the metal oxide solution is less able to reach the inside of the structure [27].

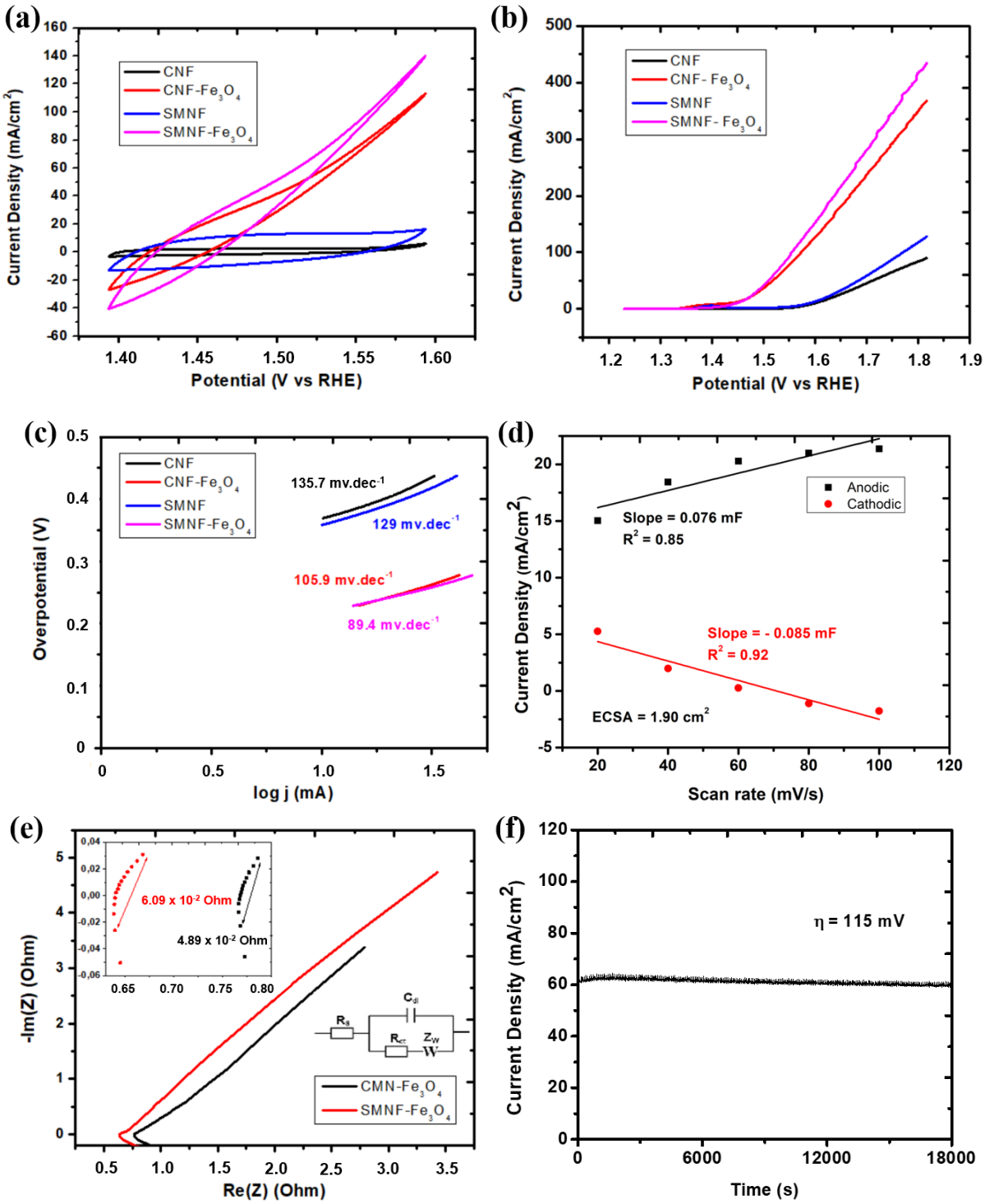

Fig. 6. Electrochemical analysis of Ni-Fe_3O_4 based electrode; (a) CV curve at the scan rate value of 100 mV s^{-1}, (b) LSV curve at the scan rate value of 2 mV s^{-1}, (c) Tafel plot of electrode SMNF-Fe_3O_4, (d) CdI graph of the SMNF-Fe_3O_4 electrode, (e) EIS comparison of CNF-Fe_3O_4 and SMNF-Fe_3O_4 electrode, (f) Chronopotentioamperometry of SMNF-Fe_3O_4 electrode.

Fig. 6(c) shows the Tafel plot results from LSV data processing. In line with the LSV results, the Tafel plot also shows that the influence of Fe_3O_4 is more significant than the porosity itself. Without adding the metal oxide, CNF and SMNF show the overpotential of 135.7mV.dec^{-1} and 129mV.dec$^{-1,}$ respectively, at the log current density of about 1 mA. The closeness of the curve positions on the CNF and SMNF electrodes shows that these two electrodes have similar chemical reactions. This close position also occurs in electrodes with the addition of active materials that have similar behaviour. Adding metal oxide as a catalyst shifted the overpotential to 105.9 mV.dec^{-1} and 89.4 mV.dec^{-1} for the CNF and SMNF, respectively. Changes in the reaction before and after adding Fe_3O_4 are the main trigger for changes in reaction kinetics in redox reactions [8].

To analyze the effect of the active surface area in electrolysis (especially in the OER process), the theoretical active surface area (ECSA) is calculated using a double-layer capacitance (CdI) plot, as shown in Fig. 6(d). This calculation is only carried out on the electrode SMNF-Fe_3O_4, which performs best. These results are then used to display the anodic and cathodic currents logarithmically and then to estimate the size of the area contributing to the reaction by comparing it with the specific capacitance. In this plot model, only anodic current was used in this study because only OER that occurred at the anode was calculated. As mentioned in the experimental section, this research accommodates the value of specific capacitance about 0.040 mF cm^{-2}, according to Connor's finding [21]. The results of measurements on the SMNF-Fe_3O_4 electrode show a slope of 0.076 mF with an ECSA value of approximately 1.90cm^2, slightly better than other research work on commercial nickel foam structures with an ECSA of 1.19cm^2[28]. This small surface area shows that efforts to maximize the surface area still have an excellent opportunity to increase the efficiency of separating O_2 from H_2O.

To complete the study of the impact of differences in SMNF and CNF porosity along with the effect of active mass loading on electrode performance, electro-impedance spectroscopy(EIS) testing was carried out on both, as depicted in Fig. 6(e). In general, there is no significant difference in the results of the impedance spectroscopy test. The spectroscopy curve shows a minuscule semicircle shape with a 45-degree line, which indicates the cell type where polarization is due to a mix of kinetic and diffusion processes [29]. The three-electrode test was modelled as a Randle circuit with R_s + (CdI/ (R_{ct}+W) to measure the outcomes of the impedance spectroscopy measurement. The R_s or solution resistance, or in some literature also known as electrical series resistance (ESR), represents the total internal resistance of the system/cell, the CdI represents the double-layer capacitance effect, the R_{ct} describes the value of charge transfer resistance between the electrodes and the solution interface, and the W represents the Warburg impedance, which represents the ion diffusion resistance. From this graph, we can see significant differences in impedance between the SMNF-Fe_3O_4 and CNF-Fe_3O_4 electrodes. Graph measurements with the help of Z fit software show that R_s in SMNF-Fe_3O_4 is about 0.638 Ω, lower than CNF- Fe_3O_4 at around 0.767 Ω. This fact shows that SMNF – Fe_3O_4 electrode with higher active surface area performs better in electrocatalyst application than commercial nickel foam.

Furthermore, the inserted picture in Fig. 6(e) shows the different values of R_{ct} in both porous structures, which is indicated by the diameter of curves in high frequency. SMNF-Fe_3O_4 electrode shows higher R_{ct} with 6.09 x 10^{-2} Ω than CNF-Fe_3O_4 with 4.89 x 10^{-2} Ω. The charge transfer resistance value for both structures is small, which indicates that the structure has good electrical contact and conductivity, which is suitable for the water-splitting process[25]. For the last part, Fig. 6(f) shows the SMNF-Fe_3O_4 electrode stability test results at an overpotential of 115 mV for 5 hours. The results are encouraging, as the current density response is stable at 60 mA cm^{-2}. Even though the voltage applied in the electrode stability test is still far below for commercial applications (usually 1.8-2.0 V) [11], the electrode's good response shows that the laser calcination technique is quite good and reliable for calcining metal oxide on Ni porous structures. This good electrode response dismisses concerns because, in several previous reports [7], the coating technique could not provide stability when applying Fe oxide to the porous Ni structure. However, we can understand that the results are still not as good as when using the alloy technique, which chemically combines Ni and Fe elements. On the other hand, adding binder in the dip coating process must be considered to form a strong bond between the porous Ni substrate and the Fe_3O_4 catalyst.

Conclusion

1. Self-manufactured nickel foam has a larger electrochemical surface area than commercial nickel foam. This large surface area can directly increase the mass loading of active material, and the redox process runs more optimally. However, in this research, the structure does not have a significant effect due to minimum active mass loading differences (< 5 mg). This low effect is caused by closed pores in porous structures, which limit access for metal oxide catalyst(Fe_3O_4) to bind with Ni substrate and electrolyte access during performance tests.

2. By previous estimates, the presence of Fe_3O_4 catalyst brings quite significant changes in the properties of the Ni electrode. Adding Fe_3O_4 decreases the overpotential on the OER from 361.4 mV to 217.3 mV in 1 M KOH at a current density value of 10 mA. Observations by chronoamperometry test at an overpotential of 155 mV at 5 hours show the stable performance of SMNF-Fe_3O_4 electrodes, which shows that the laser calcination technique has promising opportunities for thin coating processes.

References

[1] C. Tarhan and M. A. Çil, "A study on hydrogen, the clean energy of the future: Hydrogen storage methods," *J. Energy Storage*, vol. 40, no. May, p. 102676, 2021, doi: 10.1016/j.est.2021.102676.

[2] L. S. Jensen, C. Kaul, N. B. Juncker, M. H. Thomsen, and T. Chaturvedi, "Biohydrogen Production in Microbial Electrolysis Cells Utilizing Organic Residue Feedstock: A Review," *Energies*, vol. 15, no. 22, 2022, doi: 10.3390/en15228396.

[3] P. Liu *et al.*, "ScienceDirect A superhydrophilic NiFe electrode for industrial alkaline water electrolysis," *Int. J. Hydrogen Energy*, no. xxxx, 2023, doi: 10.1016/j.ijhydene.2023.07.253.

[4] A. M. Sulaiman, S. Mas'ud, A. N. Daroini, and P. Purnami, "the Effect of Electrode Coating From Bisphenol-a-Polycarbonate Cd-R Waste for Hydrogen Production," *Int. J. Mech. Eng. Technol. Appl.*, vol. 4, no. 1, pp. 10–21, 2023, doi: 10.21776/mechta.2023.004.01.2.

[5] S. Mas'ud, A. M. Sulaiman, H. Syahputra, and P. Purnami, "the Effect of Addition Bisphenol-a-Polycarbonate From Cd-R Waste As a Catalyst for Hydrogen Production," *Int. J. Mech. Eng. Technol. Appl.*, vol. 4, no. 2, pp. 104–116, 2023, doi: 10.21776/mechta.2023.004.02.1.

[6] X. Xu, Z. Shao, and S. P. Jiang, "High-Entropy Materials for Water Electrolysis," *Energy Technol.*, vol. 10, no. 11, 2022, doi: 10.1002/ente.202200573.

[7] M. Praveen Kumar *et al.*, "NiFe Layered Double Hydroxide Electrocatalyst Prepared via an Electrochemical Deposition Method for the Oxygen Evolution Reaction," *Catalysts*, vol. 12, no. 11, 2022, doi: 10.3390/catal12111470.

[8] J. Zhao, J. J. Zhang, Z. Y. Li, and X. H. Bu, "Recent Progress on NiFe-Based Electrocatalysts for the Oxygen Evolution Reaction," *Small*, vol. 16, no. 51, pp. 1–23, 2020, doi: 10.1002/smll.202003916.

[9] P. Xiong *et al.*, "Interface modulation of two-dimensional superlattices for efficient overall water splitting," *Nano Lett.*, vol. 19, no. 7, pp. 4518–4526, 2019, doi: 10.1021/acs.nanolett.9b01329.

[10] J. Mohammed-Ibrahim, "A review on NiFe-based electrocatalysts for efficient alkaline oxygen evolution reaction," *J. Power Sources*, vol. 448, no. September, p. 227375, 2020, doi: 10.1016/j.jpowsour.2019.227375.

[11] A. Kumar and S. Bhattacharyya, "Porous NiFe-Oxide Nanocubes as Bifunctional Electrocatalysts for Efficient Water-Splitting," *ACS Appl. Mater. Interfaces*, vol. 9, no. 48, pp. 41906–41915, 2017, doi: 10.1021/acsami.7b14096.

[12] Z. Angeles-Olvera, A. Crespo-Yapur, O. Rodríguez, J. L. Cholula-Díaz, L. M. Martínez, and M. Videa, *Nickel-Based Electrocatalysts for Water Electrolysis*, vol. 15, no. 5. 2022.

[13] V. Vij *et al.*, "Nickel-based electrocatalysts for energy-related applications: Oxygen reduction, oxygen evolution, and hydrogen evolution reactions," *ACS Catal.*, vol. 7, no. 10, pp. 7196–7225, 2017, doi: 10.1021/acscatal.7b01800.

[14] M. Gong, D.Y. Wang, C.C. Chen, B.J. Hwang, and H. Dai, "A mini review on nickel-based electrocatalysts for alkaline hydrogen evolution reaction," *Nano Res.*, vol. 9, no. 1, pp. 28–46, 2016, doi: 10.1007/s12274-015-0965-x.

[15] M. Gong *et al.*, "An advanced Ni-Fe layered double hydroxide electrocatalyst for water oxidation," *J. Am. Chem. Soc.*, vol. 135, no. 23, pp. 8452–8455, 2013, doi: 10.1021/ja4027715.

[16] F. Si *et al.*, "NiFe-LDH nanosheets with high activity in three dimensions on NiFe foam electrode for water oxidation," *Int. J. Hydrogen Energy*, no. xxxx, 2023, doi: 10.1016/j.ijhydene.2023.07.024.

[17] O. Diaz-Morales, I. Ledezma-Yanez, M. T. M. Koper, and F. Calle-Vallejo, "Guidelines for the Rational Design of Ni-Based Double Hydroxide Electrocatalysts for the Oxygen Evolution Reaction," *ACS Catal.*, vol. 5, no. 9, pp. 5380–5387, 2015, doi: 10.1021/acscatal.5b01638.

[18] A. Sakamaki, M. Yoshida-Hirahara, H. Ogihara, and H. Kurokawa, "One-Step Synthesis of Highly Active NiFe Electrocatalysts for the Oxygen Evolution Reaction," *Langmuir*, 2022, doi: 10.1021/acs.langmuir.2c00097.

[19] J.X. Yang *et al.*, "Rapid Fabrication of High-Entropy Ceramic Nanomaterials for Catalytic Reactions," *ACS Nano*, vol. 15, no. 7, pp. 12324–12333, 2021, doi: 10.1021/acsnano.1c04259.

[20] C.C.L. McCrory, S. Jung, J.C. Peters, and T.F. Jaramillo, "Benchmarking heterogeneous electrocatalysts for the oxygen evolution reaction," *J. Am. Chem. Soc.*, vol. 135, no. 45, pp. 16977–16987, 2013, doi: 10.1021/ja407115p.

[21] P. Connor, J. Schuch, B. Kaiser, and W. Jaegermann, "The Determination of Electrochemical Active Surface Area and Specific Capacity Revisited for the System MnOx as an Oxygen Evolution Catalyst," *Zeitschrift fur Phys. Chemie*, vol. 234, no. 5, pp. 979–994, 2020, doi: 10.1515/zpch-2019-1514.

[22] M. S. Islam, J. Kurawaki, Y. Kusumoto, M. Abdulla-Al-Mamun, and M. Z. Bin Mukhlish, "Hydrothermal Novel Synthesis of Neck-structured Hyperthermia-suitable Magnetic (Fe_3O_4, γ-Fe_2O_3 and α-Fe_2O_3) Nanoparticles," *J. Sci. Res.*, vol. 4, no. 1, p. 99, 2011, doi: 10.3329/jsr.v4i1.8727.

[23] L. Agusu, Alimin, L. O. Ahmad, M. Z. Firihu, S. Mitsudo, and H. Kikuchi, "Crystal and microstructure of MnFe2O4 synthesized by ceramic method using manganese ore and iron sand as raw materials," *J. Phys. Conf. Ser.*, vol. 1153, no. 1, pp. 2–9, 2019, doi: 10.1088/1742-6596/1153/1/012056.

[24] K. A. M. Ahmed, Q. Zeng, K. Wu, and K. Huang, "Mn3O4 nanoplates and nanoparticles: Synthesis, characterization, electrochemical and catalytic properties," *J. Solid State Chem.*, vol. 183, no. 3, pp. 744–751, 2010, doi: 10.1016/j.jssc.2010.01.015.

[25] L. Cai *et al.*, "Active site engineering of Fe- and Ni-sites for highly efficient electrochemical overall water splitting," *J. Mater. Chem. A*, vol. 6, no. 43, pp. 21445–21451, 2018, doi: 10.1039/C8TA08217K.

[26] L. Trotochaud, S. L. Young, J. K. Ranney, and S. W. Boettcher, "Nickel-Iron oxyhydroxide oxygen-evolution electrocatalysts: The role of intentional and incidental iron incorporation," *J. Am. Chem. Soc.*, vol. 136, no. 18, pp. 6744–6753, 2014, doi: 10.1021/ja502379c.

[27] M.M. Sk, C.Y. Yue, K. Ghosh, and R.K. Jena, “Review on advances in porous nanostructured nickel oxides and their composite electrodes for high-performance supercapacitors,” *J. Power Sources*, vol. 308, pp. 121–140, 2016, doi: 10.1016/j.jpowsour.2016.01.056.

[28] E. Cossar, M. S. E. Houache, Z. Zhang, and E. A. Baranova, “Comparison of electrochemical active surface area methods for various nickel nanostructures,” *J. Electroanal. Chem.*, vol. 870, p. 114246, 2020, doi: 10.1016/j.jelechem.2020.114246.

[29] B. A. Mei, O. Munteshari, J. Lau, B. Dunn, and L. Pilon, “Physical Interpretations of Nyquist Plots for EDLC Electrodes and Devices,” *J. Phys. Chem. C*, vol. 122, no. 1, pp. 194–206, 2018, doi: 10.1021/acs.jpcc.7b10582.